TIPE2 protein serves as a negative regulator of phagocytosis and oxidative burst during infection

Zhaojun Wang[a,b], Svetlana Fayngerts[a], Peng Wang[a], Honghong Sun[a], Derek S. Johnson[a], Qingguo Ruan[a], Wei Guo[c], and Youhai H. Chen[a,1]

[a]Department of Pathology and Laboratory Medicine, University of Pennsylvania School of Medicine, Philadelphia, PA 19104; [b]Department of Microbiology and Parasitology, Shanghai Jiaotong University School of Medicine, Shanghai 20025, China; and [c]Department of Biology, University of Pennsylvania, Philadelphia, PA 19104

Edited by Michael J. Lenardo, National Institute of Allergy and Infectious Diseases, National Institutes of Health, Bethesda, MD, and accepted by the Editorial Board August 11, 2012 (received for review March 15, 2012)

Phagocytosis and oxidative burst are two major effector arms of innate immunity. Although it is known that both are activated by Toll-like receptors (TLRs) and Rac GTPases, how their strengths are controlled in quiescent and TLR-activated cells is not clear. We report here that TIPE2 (TNFAIP8L2) serves as a negative regulator of innate immunity by linking TLRs to Rac. TLRs control the expression levels of TIPE2, which in turn dictates the strengths of phagocytosis and oxidative burst by binding to and blocking Rac GTPases. Consequently, TIPE2 knockout cells have enhanced phagocytic and bactericidal activities and TIPE2 knockout mice are resistant to bacterial infection. Thus, TIPE2 sets the strengths of phagocytosis and oxidative burst and may be targeted to effectively control infections.

Phagocytosis and oxidative burst (or respiratory burst) are two fundamental effector mechanisms of innate immunity that work in concert to eliminate infectious microbes (1, 2). Phagocytosis allows the phagocytes of the immune system (monocytes and granulocytes) to engulf infectious microbes and to contain them in a special vacuole called a phagosome. Oxidative burst in turn injects into the vacuole reactive oxygen species (ROS) (e.g., superoxide radical and hydrogen peroxide) that kill the microbes. Deficiency in either of these innate immune mechanisms leads to immune deficiency and uncontrolled infections (3–6).

Both phagocytosis and oxidative burst are controlled by the Rac proteins of the Ras small GTPase superfamily (1–4). There are three mammalian Rac GTPases, which are designated as Rac1, Rac2, and Rac3. Small GTPases are enzymes that hydrolyze GTP. They are active when bound to GTP and inactive when bound to GDP and serve as molecular "on-and-off" switches of signaling pathways that control a wide variety of cellular processes including growth, motility, vesicle trafficking, and death (7). Rac GTPases control phagocytosis by promoting actin polymerization through their effector proteins such as p21-activated kinases (PAKs), WASP family Verprolin homology domain-containing protein (WAVE), and IQ motif containing GTPase-activating protein-1 (IQGAP1) (1). Rac GTPases also mediate ROS production by binding and activating the NADPH oxidase complex through the p67(Phox) protein (1). Rac GTPase deficiency in mice and humans leads to an immune-deficient syndrome, which is characterized by defective phagocytosis and oxidative burst, recurrent infection, and granulomas (3–6).

Although quiescent phagocytes are capable of phagocytosis and ROS production, their levels are low. Toll-like receptor (TLR) activation or microbial infection significantly up-regulates these innate immune processes (8–11). However, the mechanisms whereby microbes promote them are not well understood. TIPE2, or tumor necrosis factor-α–induced protein 8 (TNFAIP8)-like 2 (TNFAIP8L2), is a member of the TNFAIP8 family, which is preferentially expressed in hematopoietic cells (12–18). It is significantly down-regulated in patients with infectious or autoimmune disorders (15, 19). The mammalian TNFAIP8 family consists of four members: TNFAIP8, TIPE1, TIPE2, and TIPE3, whose functions are largely unknown (14, 20). We recently generated TIPE2-deficient mice and discovered that TIPE2 plays a crucial role in immune homeostasis (14). We report here that TIPE2 controls innate immunity by targeting the Rac GTPases.

Results and Discussion

TLR Stimulation and Bacterial Infection Markedly Diminish TIPE2 Expression. TIPE2 is constitutively expressed at high levels in myeloid cells (14). To explore the relationship between TIPE2 and innate immunity, we examined its expression in murine bone marrow-derived macrophages (BMDMs) before and after stimulation with different TLR ligands/agonists. Upon stimulation with lipopolysaccharide (LPS) (the TLR4 ligand), Poly(I:C) (the TLR3 agonist), and Zymosan A (the TLR2 ligand), the expression of cytokine genes (IL-6, TNFα, and IFNβ1) significantly increased; by contrast, TIPE2 expression was significantly diminished (Fig. 1*A*). Because TLRs play essential roles in pathogen recognition and innate immunity to microbes, we next challenged the BMDMs with the bacteria *Escherichia coli* and *Listeria monocytogenes*. Both bacteria significantly augmented cytokine gene expression, but inhibited that of TIPE2 (Fig. 1*B*). Similar effects were observed in the murine macrophage cell line RAW 264.7 (Fig. 1*C*). However, unlike the RAW cell line that exhibited transient TIPE2 down-regulation (21), primary BMDMs expressed markedly reduced TIPE2 mRNA (Fig. 1*D*) and protein (Fig. 1 *E* and *F*) even 16 h after LPS or bacterial challenge. These results indicate that TIPE2 may regulate the early phase of innate immune responses.

TIPE2 Binds to Rac GTPases Through Their C-Terminal CAAX Motif. To identify TIPE2-interacting proteins, we performed large-scale coimmunoprecipitation and mass spectrometry screenings using RAW 264.7 cells. Among the peptides identified, three were shared by the small GTPases Rac1 and Rac2, members of the Rho family. Both Rac1 and Rac2 are expressed in neutrophils and macrophages. They share 92% identity in primary sequences and perform crucial functions in innate immune responses (2).

To determine whether TIPE2 indeed interacts with the Rac GTPases in mammalian cells, we undertook four complementary approaches. First, we expressed Flag-tagged TIPE2 and Myc-tagged Rac1 or Rac2 in 293T cells and, by coimmunoprecipitation (co-IP) analyses, we found that TIPE2 interacted with both Rac1 and Rac2 (Fig. 2*A*). Second, we determined whether endogenous TIPE2 interacts with endogenous Rac. Murine RAW 264.7 macrophage extracts were used to immunoprecipitate Rac-

Author contributions: Z.W. and Y.H.C. designed research; Z.W., P.W., H.S., D.S.J., and Q.R. performed research; S.F. and W.G. contributed new reagents/analytic tools; Z.W. and Y.H.C. analyzed data; and Z.W. and Y.H.C. wrote the paper.

The authors declare no conflict of interest.

This article is a PNAS Direct Submission. M.J.L. is a guest editor invited by the Editorial Board.

[1]To whom correspondence should be addressed. E-mail: yhc@mail.med.upenn.edu.

This article contains supporting information online at www.pnas.org/lookup/suppl/doi:10.1073/pnas.1204525109/-/DCSupplemental.

IMMUNOLOGY

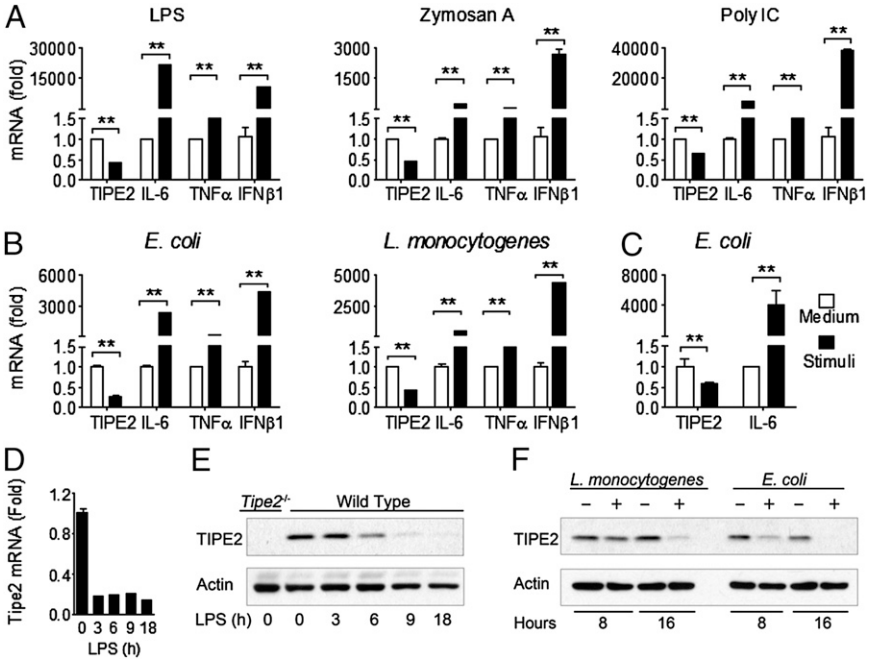

Fig. 1. TLR stimulation and bacterial infection markedly diminish TIPE2 expression. (*A*) Wild-type (WT) bone marrow-derived macrophages (BMDMs) were stimulated with lipopolysaccharide (100 ng/mL), Poly(I:C) (10 μg/mL), and Zymosan A (100 μg/mL) for 2 h. TIPE2, IL-6, TNFα, and IFNβ1 mRNA levels were determined by real-time PCR. (*B* and *C*) WT BMDMs (*B*) or RAW 264.7 cells (*C*) were infected with *Escherichia coli* or *Listeria monocytogenes* at a multiplicity of infection (MOI) of 10 for 2 h. The mRNA levels of indicated genes were determined by real-time PCR. (*D* and *E*) BMDMs from WT mice were treated with LPS for the indicated times. TIPE2 mRNA (*D*) and protein (*E*) levels were analyzed by real-time PCR and Western blot, respectively. BMDMs from TIPE2-deficient mice (*Tipe2*$^{-/-}$) were used as a control. (*F*) WT BMDMs were infected with or without the indicated bacteria for 8 or 16 h. TIPE2 protein levels were analyzed by Western blot. Statistics were performed on pooled data from three independent experiments. Error bars represent the SDs of the means. *$P < 0.05$, **$P < 0.01$.

binding proteins with anti-Rac1/2/3 polyclonal antibodies. Upon blotting with anti-TIPE2 antibody, a strong TIPE2 signal was detected in the precipitates (Fig. 2*B*), indicating that TIPE2 is constitutively associated with Rac proteins in nonstimulated immune cells. By contrast, in the same RAW cells, we did not detect any interaction between endogenous TIPE2 and several other GTPases, including Cdc42, RhoA, RalA, and HRas, suggesting that the TIPE2–Rac interaction is specific. Third, we tested whether TIPE2 and Rac might directly interact with each other. TIPE2 and Rac1 proteins were synthesized separately, using an in vitro transcription–translation system. After mixing them together, we found that TIPE2 physically associated with Rac1, indicating that the two proteins might directly bind to each other (Fig. 2 *C* and *D*). Finally, using both GDP and GTP forms of Rac1 (22, 23), we showed that TIPE2–Rac interaction was not affected by the Rac1-activating status; i.e., TIPE2 binds to both GDP and GTP forms of Rac1 (Fig. 2*E*).

To map the region within Rac that is responsible for TIPE2 interaction, we generated full-length Rac1 (amino acids 1–192) and a series of deletion constructs in frame with an HA tag (Fig. 3*A*). Among five deletion Rac1 mutants we generated, two (with amino acids 48–123 deletion and amino acids 136–161 deletion) were unstable in cells and could not be further studied. By contrast, Rac1 mutants without the N terminus (amino acids 1–47), the insert region (amino acids 124–135), or the C terminus (amino acids 162–192) were stable and therefore were used in this study. By co-IP, we found that the C terminus, but not the N terminus or the insert region, was required for TIPE2 interaction (Fig. 3*B*).

The C terminus of Rac contains a polybasic region (PBR) and a CAAX motif. To determine which of these elements is involved in TIPE2 binding, we made two additional Rac1 mutants, one without the PBR and one without the CAAX motif. By co-IP, we found that the CAAX motif, but not the PBR, was required for TIPE2 interaction (Fig. 3*C*). The cysteine residue, Cys-189, in the C-terminal CAAX motif is crucial for the posttranslational modification and function of Rac (23). Using a point mutant form of Rac1, Rac1C189S, in which Cys-189 is replaced by serine, we found that TIPE2 binding required Cys-189 (Fig. 3*D*).

TIPE2 Inhibits Rac Membrane Translocation, Rac Activation, and Downstream Rac Signaling. The hydrophobic C-terminal region of Rac is responsible for targeting and anchoring Rac to the plasma membrane. Our finding that TIPE2 binds to the C terminus of Rac suggests that it may regulate membrane translocation of Rac. To test this possibility, we transiently expressed increasing amounts of TIPE2 in 293T cells. At 8 h after transfection, TIPE2 did not induce a significant amount of cell death (Fig. S1), but reduced the membrane-bound, not the cytosolic, endogenous Rac in a dose-dependent manner (Fig. 3*E*). The TIPE2 N-terminal lysine or arginine residues, Lys-15, Lys-16, and Arg-24, are important for TIPE2–Rac1 interaction because replacing them with glutamine or alanine markedly reduced the Rac1 binding (Fig. 3*F*). By contrast, Lys-20 mutation did not affect the binding. As a consequence, the TIPE2 K15/16Q and R24A mutants were not as effective as wild-type TIPE2 in inhibiting Rac membrane translocation (Fig. 3*G*). As stated above, LPS markedly reduced TIPE2 levels in macrophages. This reduction was associated with increased Rac1 membrane translocation in LPS-treated cells (Fig. 3*H*), indicating that TIPE2 regulates Rac membrane translocation.

Because plasma membrane translocation of small GTPases is required for their activation, these results indicate that TIPE2 may regulate Rac activation. To test this hypothesis, we undertook three complementary approaches. First, using confocal microscopy and an antibody that recognized GTP-Rac but not GDP-Rac, we examined the levels of membrane-bound GTP-Rac in 293T cells that did or did not receive TIPE2 transfection. We found that 293T cells exhibited prominent endogenous GTP-Rac staining on the plasma membrane, which was significantly blocked in cells transfected with

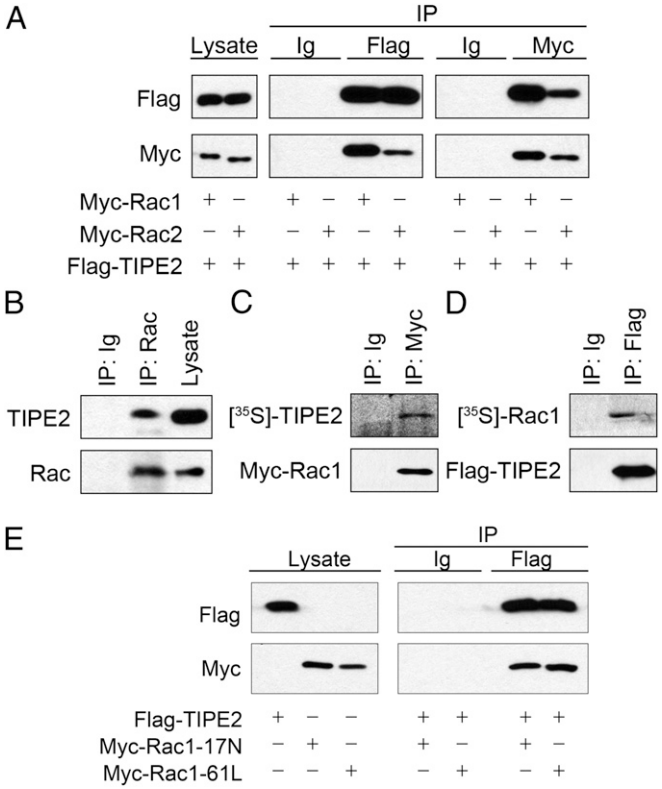

Fig. 2. TIPE2 interacts with Rac GTPase. (*A*) 293T cells were transfected with pRK5 vector or expression plasmids for Flag-tagged TIPE2 and Myc-tagged Rac1 or Rac2 as indicated. Eighteen hours later, cell lysates were prepared and immunoprecipitated with anti-Flag, anti-Myc, or control Ig. The precipitates and lysates were subjected to Western blotting with antibodies for the indicated antigens. (*B*) Total cell lysates of RAW 264.7 cells were immunoprecipitated with rabbit polyclonal anti-Rac1/2/3 or control rabbit Ig. The immunoprecipitates and cell lysates were then blotted with anti-TIPE2 or anti-Rac1/2/3. (*C*) [^{35}S]Methionine-labeled TIPE2 and unlabeled Myc-tagged Rac1 were synthesized in vitro, using the TNT transcription–translation system. The mixture was immunoprecipitated with anti-Myc or Ig control and then analyzed by SDS/PAGE and Western blotting. (*Upper*) Autoradiograph of the immunoprecipitates on SDS/PAGE; (*Lower*) anti-Myc immunoblotting result. (*D*) In vitro synthesized [^{35}S]methionine-labeled Rac1 and Flag-tagged TIPE2 mixture were immunoprecipitated with anti-Flag or control Ig and analyzed as in *C*. (*E*) 293T cells were transiently transfected with Flag-TIPE2, Myc-tagged Rac1-17N, or Rac1-61L. Eighteen hours later, lysates of Myc-Rac1-17N– and Myc-Rac1-61L–transfected cells were loaded with GDP and GTP, respectively, and mixed with lysates of Flag-TIPE2–transfected cells. After immunoprecipitation with anti-Flag or control Ig, the samples were subjected to Western blotting with antibodies for the indicated antigens. The experiments were repeated at least three times with similar results.

TIPE2, but not in cells transfected with a control GFP plasmid (Fig. 4*A*). Second, using a GST pull-down assay that specifically recognized active GTP-bound Rac, we tested the TIPE2 effect in 293T cells that did or did not express a constitutive active form of HRas (HRas12V). We found that TIPE2 transfection decreased the Rac-GTP levels in both cell types (Fig. 4*B*). Third, we tested the effect of TIPE2 deficiency on Rac activation in macrophages. We found that resting TIPE2-deficient murine macrophages exhibited an increase in active Rac levels over wild-type controls. The difference was more dramatic upon the activation of the Rac pathway with fibronectin (Fig. 4*C*). The total Rac levels were not affected by TIPE2 overexpression or deficiency, indicating that TIPE2 may not regulate Rac activity through protein expression or degradation.

A number of studies have demonstrated that Rac can activate both the c-Jun N-terminal kinase (JNK) and the PAK pathways (24). In 293T cells, we found that constitutively active Rac expression did induce JNK and PAK activation as reflected by increased phosphorylation; this effect was blocked by TIPE2 in a dose-dependent manner (Fig. 4*D*). Active Rac1 can induce the assembly of a filamentous (F)-actin structure through PAK-dependent and -independent signals (24). Because polymerization of F-actin can be induced by LPS, we next examined the effect of TIPE2 deficiency on LPS-induced F-actin polymerization. We found that in TIPE2-deficient BMDMs, the F-actin polymerization rate was significantly enhanced compared with that in wild-type cells (Fig. 4*E*). A similar phenotype was observed in TIPE2-deficient splenocytes (21).

TIPE2 Inhibits the Basal Level of Phagocytosis Through Rac, and TIPE2 Down-Regulation Contributes to TLR-Induced Augmentation of Phagocytosis. Rac proteins are key molecular switches of phagocytosis (2). To determine the roles of TIPE2 in phagocytosis, we used both TIPE2 loss-of-function and gain-of-function approaches. Thus, macrophages were first generated from WT and *Tipe2*-deficient murine bone marrow. They showed no differences in surface marker

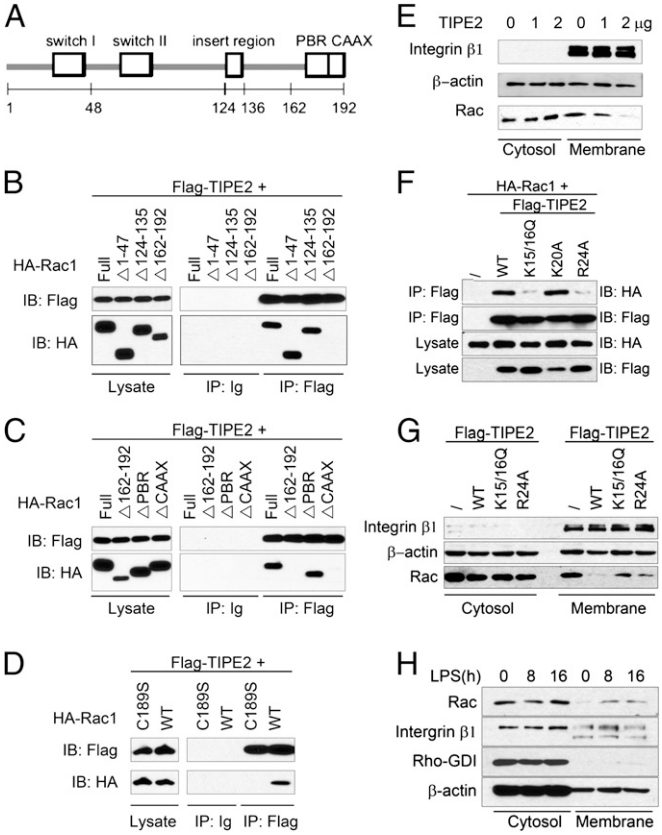

Fig. 3. TIPE2 binding to Rac requires the C-terminal CAAX motif, and TIPE2 inhibits Rac membrane translocation. (*A*) Schematic diagram of the Rac1 protein. (*B–D*) Lysates of 293T cells transiently transfected with HA-Rac1 constructs and Flag-TIPE2 construct were immunoprecipitated with anti-Flag and subjected to Western blotting. (*E*) 293T cells were transiently transfected with increasing amounts of TIPE2 plasmids for 8 h. Cell lysates were separated into membrane and cytosolic fractions. Equal amounts of cytosolic and membrane materials (3 μg) were separated by SDS/PAGE and immunoblotted for integrin β1, β-actin, and Rac. (*F*) Lysates of 293T cells transiently transfected with or without HA-Rac1 construct and Flag-TIPE2 constructs were immunoprecipitated and subjected to Western blotting. (*G*) 293T cells were transiently transfected with or without the indicated TIPE2 plasmids. Equal amounts of cytoplasmic and membrane protein fractionations were subjected to Western blotting. (*H*) WT BMDMs were treated with LPS for up to 16 h. Cytosolic and membrane protein fractionations were subjected to Western blotting. The experiments were repeated at least three times with similar results.

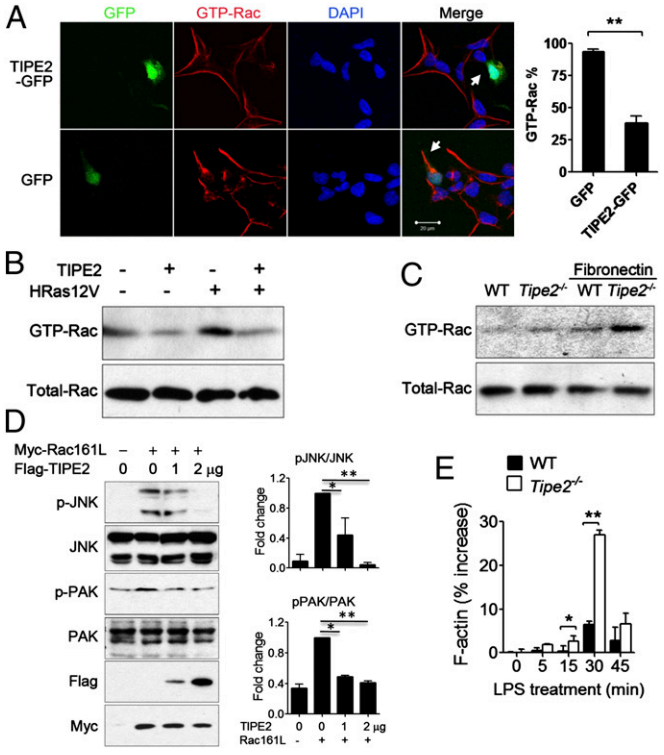

Fig. 4. TIPE2 inhibits the activation of Rac and its effectors. (*A*) Confocal microscopy of 293T cells expressing TIPE2-GFP or GFP alone. To detect active Rac, cells were stained with anti–GTP-Rac and Alexa Fluor 555-labeled goat anti-mouse Ig (red). Images are representative of three independent experiments. (*Right*) The percentages of GTP-Rac–positive cells in total GFP positive cells. A total of 70 cells were counted for each condition (*B*) 293T cells were transiently transfected with TIPE2 and/or HRas12V as indicated. Cell lysates were subjected to pull-down, using PAK-GST protein beads. Rac from the pull-down and total Rac in the lysates were detected by Western blot. (*C*) WT and *Tipe2*$^{-/-}$ BMDMs were plated on uncoated or fibronectin-coated dishes for 15 min at 37 °C. Active and total Rac levels in the cells were determined as in *B*. (*D*) 293T cells were transfected with or without Myc-Rac161L (2 μg/6-cm dish) and increasing amounts of Flag-TIPE2 constructs (1–2 μg/6-cm dish) for 8 h, and the levels of phospho(p)-JNK, total JNK, phospho(p)-PAK, total PAK, Myc, and Flag were determined by Western blot. Bar graphs show relative p-JNK and p-PAK levels as determined by densitometry. (*E*) WT and *Tipe2*$^{-/-}$ BMDMs were treated with LPS (100 ng/mL) for the indicated times and F-actin level was measured as described in *Methods*. The "% increase in F-actin" = [(F-actin in LPS-treated cells − F-actin in untreated cells)/F-actin in untreated cells] × 100. Results are means ± SEM. Statistics were performed on pooled data from three independent experiments. **P* < 0.05, ***P* < 0.01.

expression (Fig. S2). They were then fed with apoptotic thymocytes from GFP transgenic mice. Thirty minutes later, the engulfment of GFP-positive cells was measured by flow cytometry. Remarkably, TIPE2 deficiency increased the basal phagocytosis rate by approximately twofold (Fig. 5*A*). Moreover, the mean fluorescence intensity of *Tipe2*-deficient GFP-positive cells was also significantly increased. Addition of the actin polymerization inhibitor, cytochalasin B, markedly reduced phagocytosis in both WT and *Tipe2*$^{-/-}$ groups, indicating that actin remodeling is required and that TIPE2 may regulate internalization rather than adherence (Fig. 5*A*). The increased phagocytic activity of *Tipe2*-deficient cells was not restricted to apoptotic cells, because *Tipe2*-deficient macrophages were significantly more active in engulfing fluorescently labeled 2-μm beads (Fig. 5*B*) and live or dead bacteria (Fig. 5*C*). The increase in phagocytosis of *Tipe2*-deficient cells was not affected by the culture media used [with or without 10% (vol/vol) fetal bovine sera or freshly prepared murine sera that contain different amounts of Ig and/or complements], indicating that the TIPE2 effect on phagocytosis may not be dependent on Fc or complement receptor use (Fig. S3). In contrast to phagocytosis, endocytosis of fluorescence-labeled dextran was not affected by TIPE2 deficiency (Fig. S4).

To directly test the effect of TIPE2 on phagocytosis, we overexpressed TIPE2 in WT and *Tipe2*$^{-/-}$ macrophages. In *Tipe2*$^{-/-}$ cells, ectopic TIPE2 reduced phagocytosis by more than fourfold, whereas in WT cells that constitutively expressed high levels of

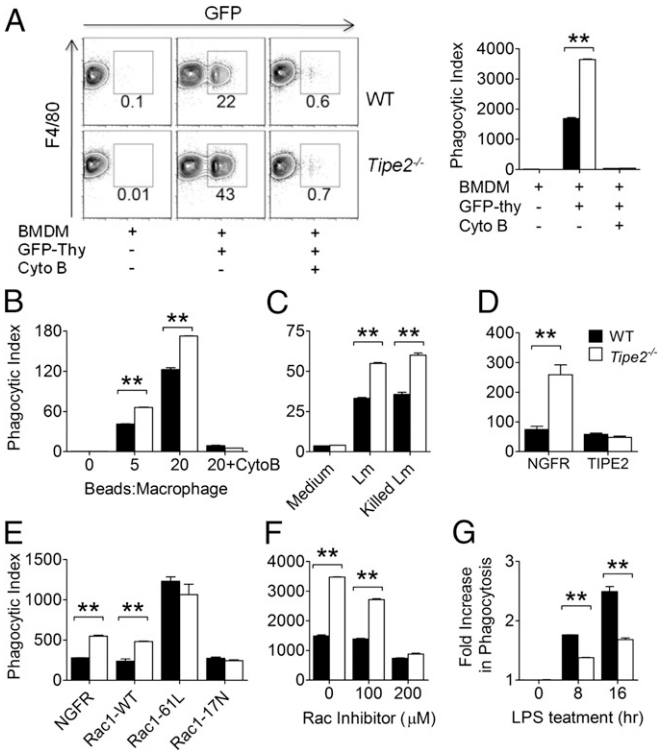

Fig. 5. TIPE2 controls the strength of phagocytosis through Rac. (*A*) BMDMs from WT and *Tipe2*$^{-/-}$ mice were incubated with or without apoptotic GFP thymocytes (GFP-Thy) for 30 min at a ratio of 1:5. One group of BMDMs was also pretreated with 5 μM Cytochalasin B (Cyto B) for 5 min as indicated. After incubation, cells were fixed, stained with an antibody to the macrophage marker F4/80, and analyzed by flow cytometry. Only cells in the macrophage gates set based on the FSC/SSC values are shown. The number in each contour plot represents the percentage of GFP^{+}F4/80^{+} cells (macrophages with ingested thymocytes) in the gated area. Solid bar, WT BMDMs; open bar, *Tipe2*$^{-/-}$ BMDMs. Phagocytic index = the percentage of gated fluorescent macrophages × mean fluorescence intensity of gated macrophages. (*B* and *C*) WT (solid bars) and *Tipe2*$^{-/-}$ BMDMs (open bars) were fed with 2-μm fluorescent beads at the indicated ratio with or without Cyto B (*B*) or CFSE-labeled live or heat-killed *L. monocytogenes* (Lm) at a ratio of 1:10 (*C*) and incubated for 20 min. Phagocytic indexes were determined as in *A*. (*D*) WT and *Tipe2*$^{-/-}$ BMDMs were infected with retroviruses that carried either nerve growth factor receptor (NGFR) or NGFP plus TIPE2 cDNAs (TIPE2) as described in *Methods*. Phagocytic indexes were determined as in *A*. Only data from NGFR-positive macrophages are shown. (*E*) WT (solid bars) and *Tipe2*$^{-/-}$ BMDMs (open bars) were infected with retroviruses that carried NGFR or NGFP plus wild-type Rac1 (Rac1-WT), constitutively active Rac1 (Rac1-61L), or dominant-negative Rac1 (Rac1-17N) cDNAs. Phagocytic indexes were determined as in *A*. Only data from NGFR-positive macrophages are shown. (*F*) WT (solid bars) and *Tipe2*$^{-/-}$ BMDMs (open bars) were pretreated with Rac1 inhibitor NSC24766 at the indicated concentrations for 24 h and incubated with GFP-Thy for 30 min at a ratio of 1:5. Phagocytosis index was determined as in *A*. (*G*) WT (solid bars) and *Tipe2*$^{-/-}$ BMDMs (open bars) were treated with LPS (100 ng/mL) for the indicated times. After the treatment, cells were subjected to the phagocytosis assay as in *A*. The fold increase in the phagocytic index is shown, with the value of the untreated cells set as 1. Results shown are means ± SEM. Statistics were performed on pooled data from three independent experiments. ***P* < 0.01.

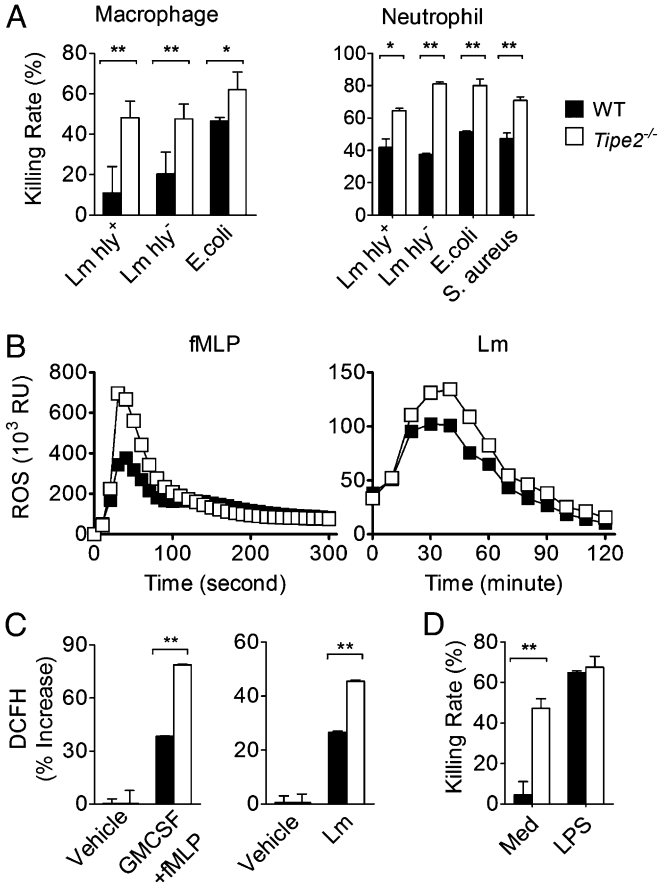

Fig. 6. TIPE2 controls the oxidative burst and bactericidal activity. (*A*) BMDMs and neutrophils from WT and *Tipe2*$^{-/-}$ mice were infected with wild-type (hly^{+}) or hly mutant (hly^{-}) *L. monocytogenes* (Lm), *E. coli*, *or S. aureus*, at a ratio of 1:1 for 20 min. After washing, cells were incubated for an additional 2 h. Bacterial numbers in the cells were determined by the colony-forming unit assay both before and after the 2-h incubation period. (*B*) Neutrophils from WT (solid squares) and *Tipe2*$^{-/-}$ mice (open squares) were stimulated with 5 μM fMLP or *L. monocytogenes* (Lm) at MOI of 10. Total ROS responses were measured by the chemiluminescence assay as described in *Methods*. Data shown are profiles of the kinetics of ROS production, from one representative experiment of four. RU, relative units. The differences at the peak light production time points between the two groups are statistically significant as determined by Student's *t* test ($P < 0.01$). (*C*) Neutrophils from WT (solid bars) and *Tipe2*$^{-/-}$ mice (open bars) were treated with GM-CSF (10 ng/mL) and fMLP (1 μM) or infected with *L. monocytogenes* at a ratio of 1:5. Intracellular ROS levels were measured by DCFDA (DCFH) staining. (*D*) BMDMs from WT (solid bars) and *Tipe2*$^{-/-}$ mice (open bars) were treated with or without LPS (100 ng/mL) for 24 h. After the treatment, bactericidal activity was measured as in *A*. Results shown are means ± SEM and are pooled from three to six independent experiments. *$P < 0.05$, **$P < 0.01$.

TIPE2 it had a much smaller effect (Fig. 5*D* and Fig. S5). Importantly, ectopic TIPE2 completely eliminated the augmented phagocytic activity of *Tipe2*$^{-/-}$ cells compared with WT cells.

To determine whether TIPE2 regulates phagocytosis through Rac, we manipulated the Rac activity using Rac mutants and chemical blockers. Expression of a constitutively active Rac (61L) dramatically increased phagocytosis in both WT and *Tipe2*$^{-/-}$ macrophages and abolished the difference between them. On the other hand, dominant-negative Rac1 (17N) significantly reduced phagocytosis in *Tipe2*$^{-/-}$ cells and eliminated the difference between WT and *Tipe2*$^{-/-}$ cells (Fig. 5*E* and Fig. S6). Similarly, the Rac1 antagonist NSC23766 depressed the ability of macrophages to uptake apoptotic cells and reduced the difference between WT and *Tipe2*$^{-/-}$ groups in a dose-dependent manner (Fig. 5*F*).

The basal level of phagocytosis is significantly increased upon TLR activation (8, 9). Because TLRs down-regulate TIPE2 expression, we asked whether TLRs augment phagocytosis through TIPE2. WT and *Tipe2*$^{-/-}$ macrophages were therefore stimulated with LPS and their phagocytic ability was tested. As reported, LPS stimulation enhanced phagocytosis of WT cells in a time-dependent manner. However, this enhancement was significantly reduced in *Tipe2*$^{-/-}$ cells (Fig. 5*G* and Fig. S7). These results indicate that TIPE2 down-regulation contributes to the TLR-induced increase in phagocytosis.

TIPE2 Inhibits Oxidative Burst, and Its Down-Regulation Contributes to TLR-Induced Augmentation of Bactericidal Activity. Because Rac proteins are crucial for assembling the NADPH complex and for producing ROS, we next investigated whether TIPE2 regulates ROS production and bacterial killing. We found that *Tipe2*$^{-/-}$ macrophages exhibited enhanced bacterial clearance within 2 h of bacterial infection. They killed *L. monocytogenes* and *E. coli* more efficiently than WT macrophages. Similar differences were observed between *Tipe2*$^{-/-}$ and WT neutrophils (Fig. 6*A*).

We then assessed ROS production in bone marrow neutrophils of WT and *Tipe2*$^{-/-}$ mice, using a horseradish peroxidase (HRP)-dependent chemiluminescence assay. *N*-formyl-methionyl-leucyl-phenylalanine (fMLP), a bacterial peptide, and *L. monocytogenes* were used to induce ROS production. Compared with WT cells, *Tipe2*$^{-/-}$ neutrophils exhibited significantly enhanced ROS production after

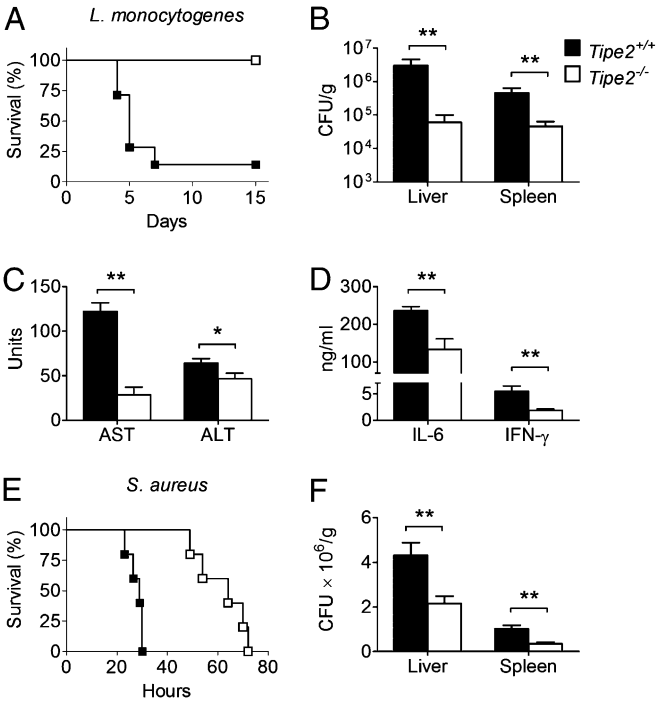

Fig. 7. *Tipe2*$^{-/-}$ mice are resistant to *L. monocytogenes* and *S. aureus* infection. (*A*) Survival rate of WT and *Tipe2*$^{-/-}$ mice ($n = 7$) infected with 2×10^5 cfus of *L. monocytogenes* (Lm) via the tail vein. The difference between the two groups is statistically significant ($P < 0.01$). (*B*) The numbers of bacteria in the spleen and liver of individual mice were determined on day 3 by colony-forming unit assay. (*C*) Levels of serum aspartate transaminase (AST) and alanine transaminase (ALT) on day 3. (*D*) One day after the infection, serum cytokines were determined by ELISA. Error bars represent the SDs of the means. (*E*) Survival rate of WT and *Tipe2*$^{-/-}$ mice ($n = 9$) infected with *S. aureus* (6×10^7 cfus/mouse) via the tail vein. (*F*) Bacterial titers were assayed at 24 h after i.v. inoculation of *S. aureus* (2×10^7 cfus/mouse). Statistics were performed on pooled data from two independent experiments. *$P < 0.05$, **$P < 0.01$.

IMMUNOLOGY

stimulation (Fig. 6*B*). Intracellular ROS levels were then measured in the dichlorofluorescin diacetate (DCFDA) assay (Fig. 6*C*). GM-CSF priming and fMLP stimulation triggered significantly more ROS production in *Tipe2*$^{-/-}$ cells than in WT cells. Similarly, when cells were challenged with *Listeria*, more ROS were detected in *Tipe2*$^{-/-}$ neutrophils than in WT neutrophils. Intracellular ROS production was also tested by luminol-dependent luminescence assay in the absence of HRP. Again, significant differences in the ROS production between *Tipe2*$^{-/-}$ and WT neutrophils were observed (Fig. S8).

TLR activation increases the bactericidal activity of macrophages (25, 26). We next investigated whether TIPE2 down-regulation contributes to LPS-induced enhancement of bacterial killing. We found that LPS stimulation significantly enhanced the killing ability of WT macrophages. By contrast, the LPS effect was markedly reduced in *Tipe2*$^{-/-}$ cells, indicating that TIPE2 is involved in the LPS-induced regulation of bacterial killing (Fig. 6*D*).

TIPE2-Deficient Mice Are Resistant to Bacterial Infection. In vitro, down-regulation of TIPE2 is associated with increased phagocytosis and bacterial killing. To assess the in vivo relevance of these findings, we infected *Tipe2*$^{-/-}$ and WT mice with a lethal dose of *L. monocytogenes* (Fig. 7*A*). More than 80% of WT mice succumbed within 7 d after infection, whereas all *Tipe2*$^{-/-}$ mice survived ($P < 0.01$). The increased mortality of WT mice was associated with enhanced bacteria growth, tissue damage, and cytokine production. At day 3 postinfection, the *Listeria* titer in the liver and spleen of WT mice was significantly higher than that in *Tipe2*$^{-/-}$ mice (Fig. 7*B*). The blood alanine transaminase (ALT) and aspartate transaminase (AST) levels are indicators of hepatic injury. After *Listeria* infection, the blood ALT and AST levels were significantly higher in WT than in *Tipe2*$^{-/-}$ mice (Fig. 7*C*). Fewer serum inflammatory cytokines were detected in *Tipe2*$^{-/-}$ mice compared with WT mice (Fig. 7*D*). Additionally, we also challenged the *Tipe2*$^{-/-}$ and WT mice with *Staphylococcus aureus*. Consistent with the *Listeria* experiment, *Tipe2*$^{-/-}$ mice survived for a longer time and carried significantly fewer bacteria in their liver and spleen (Fig. 7 *E* and *F*). Taken together, these results demonstrate that TIPE2 inhibits immunity to bacteria.

Methods

Mice. C57BL/6 mice that carry a *Tipe2* gene null mutation were generated by backcrossing *Tipe2*$^{-/-}$ 129 mice to C57BL/6 (B6) mice for 12 generations.

Methods. The following methods are described in *SI Methods*: plasmid constructs; cell culture and transfection; macrophage generation and neutrophil isolation; gene transfer in primary macrophages; microbial strains and infection; real-time quantitative PCR; protein extraction, cell subcellular fractionation, and immunoblotting; cell lysate preparation, protein in vitro translation, and immunoprecipitation; loading of Rac1 with GDP and GTP; immunofluorescence and confocal microscopy; PBD pull-down assay; F-actin determination; phagocytosis assay; determination of bactericidal activity; detection of ROS; ELISA; and statistical analyses.

ACKNOWLEDGMENTS. The authors thank Drs. H. Shen and Y. Paterson (University of Pennsylvania) for providing *L. monocytogenes* and Dr. Y. Fan (Shandong University) for rabbit anti-TIPE2. This work was supported by National Institutes of Health Grants AI-077533, AI-050059, and GM-085112.

1. Diebold BA, Bokoch GM (2005) Rho GTPases and the control of the oxidative burst in polymorphonuclear leukocytes. *Curr Top Microbiol Immunol* 291:91–111.
2. Niedergang F, Chavrier P (2005) Regulation of phagocytosis by Rho GTPases. *Curr Top Microbiol Immunol* 291:43–60.
3. Ambruso DR, et al. (2000) Human neutrophil immunodeficiency syndrome is associated with an inhibitory Rac2 mutation. *Proc Natl Acad Sci USA* 97:4654–4659.
4. Roberts AW, et al. (1999) Deficiency of the hematopoietic cell-specific Rho family GTPase Rac2 is characterized by abnormalities in neutrophil function and host defense. *Immunity* 10:183–196.
5. Heyworth PG, Cross AR, Curnutte JT (2003) Chronic granulomatous disease. *Curr Opin Immunol* 15:578–584.
6. Assari T (2006) Chronic granulomatous disease; fundamental stages in our understanding of CGD. *Med Immunol* 5:4.
7. Colicelli J (2004) Human RAS superfamily proteins and related GTPases. *Sci STKE* 2004: RE13.
8. Blander JM, Medzhitov R (2004) Regulation of phagosome maturation by signals from toll-like receptors. *Science* 304:1014–1018.
9. Takeda K, Akira S (2005) Toll-like receptors in innate immunity. *Int Immunol* 17:1–14.
10. Kong L, Ge BX (2008) MyD88-independent activation of a novel actin-Cdc42/Rac pathway is required for Toll-like receptor-stimulated phagocytosis. *Cell Res* 18: 745–755.
11. Tricker E, Cheng G (2008) With a little help from my friends: Modulation of phagocytosis through TLR activation. *Cell Res* 18:711–712.
12. Ahn SH, et al. (2010) Two genes on A/J chromosome 18 are associated with susceptibility to Staphylococcus aureus infection by combined microarray and QTL analyses. *PLoS Pathog* 6:e1001088.
13. Laliberté B, et al. (2010) TNFAIP8: A new effector for Galpha(i) coupling to reduce cell death and induce cell transformation. *J Cell Physiol* 225:865–874.
14. Sun H, et al. (2008) TIPE2, a negative regulator of innate and adaptive immunity that maintains immune homeostasis. *Cell* 133:415–426.
15. Li D, et al. (2009) Down-regulation of TIPE2 mRNA expression in peripheral blood mononuclear cells from patients with systemic lupus erythematosus. *Clin Immunol* 133:422–427.
16. Zhang X, et al. (2009) Crystal structure of TIPE2 provides insights into immune homeostasis. *Nat Struct Mol Biol* 16:89–90.
17. Zhang G, et al. (2010) Tissue-specific expression of TIPE2 provides insights into its function. *Mol Immunol* 47:2435–2442.
18. Zhang S, et al. (2010) Expression and regulation of a novel identified TNFAIP8 family is associated with diabetic nephropathy. *Biochim Biophys Acta* 1802:1078–1086.
19. Xi W, et al. (2011) Roles of TIPE2 in hepatitis B virus-induced hepatic inflammation in humans and mice. *Mol Immunol* 48:1203–1208.
20. Zhang C, et al. (2006) Role of SCC-S2 in experimental metastasis and modulation of VEGFR-2, MMP-1, and MMP-9 expression. *Mol Ther* 13:947–955.
21. Gus-Brautbar Y, et al. (2012) The anti-inflammatory TIPE2 is an inhibitor of the oncogenic Ras. *Mol Cell* 45:610–618.
22. Hirshberg M, Stockley RW, Dodson G, Webb MR (1997) The crystal structure of human rac1, a member of the rho-family complexed with a GTP analogue. *Nat Struct Biol* 4: 147–152.
23. Kreck ML, Uhlinger DJ, Tyagi SR, Inge KL, Lambeth JD (1994) Participation of the small molecular weight GTP-binding protein Rac1 in cell-free activation and assembly of the respiratory burst oxidase. Inhibition by a carboxyl-terminal Rac peptide. *J Biol Chem* 269:4161–4168.
24. Kreis P, Barnier JV (2009) PAK signalling in neuronal physiology. *Cell Signal* 21: 384–393.
25. West AP, et al. (2011) TLR signalling augments macrophage bactericidal activity through mitochondrial ROS. Nature 472:476–480.
26. Henneke P, et al. (2002) Cellular activation, phagocytosis, and bactericidal activity against group B streptococcus involve parallel myeloid differentiation factor 88-dependent and independent signaling pathways. *J Immunol* 169:3970–3977.